Ionization and Separation as A Strategy for Significantly Enhancing the Thermal Stability of An Instable System: A Case of Hydroxylamine-based Salts Relative to Pure Hydroxylamine

Yu Ma, Xudong He, Liya Meng, Xianggui Xue, and Chaoyang Zhang*

Institute of Chemical Materials, China Academy of Engineering Physics (CAEP), P. O. Box 919-311, Mianyang, Sichuan 621900, China.

Electronic Supplementary Information

Table of Contents

S1. Decomposition temperature of HA-based EISs.

Table S1. Decomposition temperature (in, ℃) of HA-based EISs

Anions-based EISs	T_d
BT-HA[1]	205
BT$_2$O-HA[2]	172
DBO-HA[3]	156
DNABF-HA[4]	141
DNBTO-HA[5]	217
BTO-HA[6]	221
AFTA-HA[7]	213
NTX-HA[8]	157
DNAAF-HA[9]	177
DPNA-HA[10]	166
BNT-HA[11]	218
HH[12]	152
HS[12]	177
HP[12]	148
HAP[12]	75
HN[12]	48
HA[12]	33

S2. Typical snapshots of HA with densities of 0.14 and 0.014 g/cm³ in nonreactive forcefield NVT simulations..
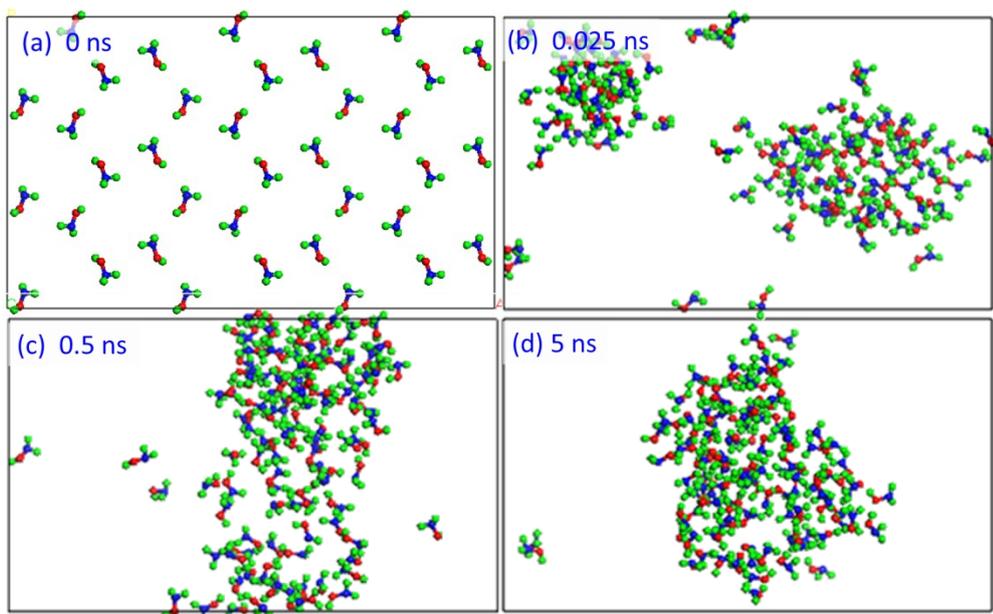
Fig. s1 Typical snapshots of NVT (T=500 K) MD simulations of HA with a density of 0.14 g/cm³.
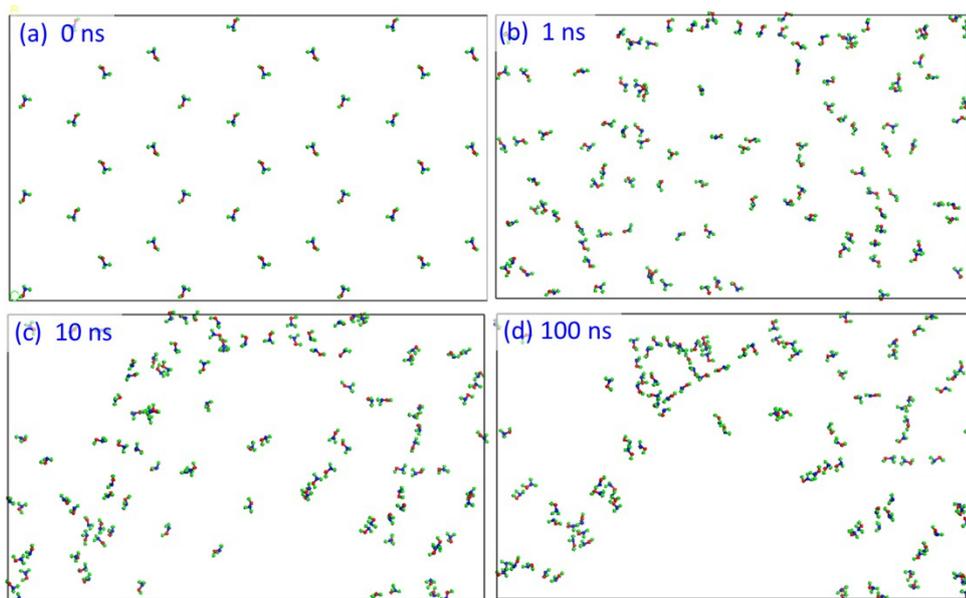
Fig. s2 Typical snapshots of NVT (T=500 K) MD simulations of HA with a density of 0.014 g/cm³.
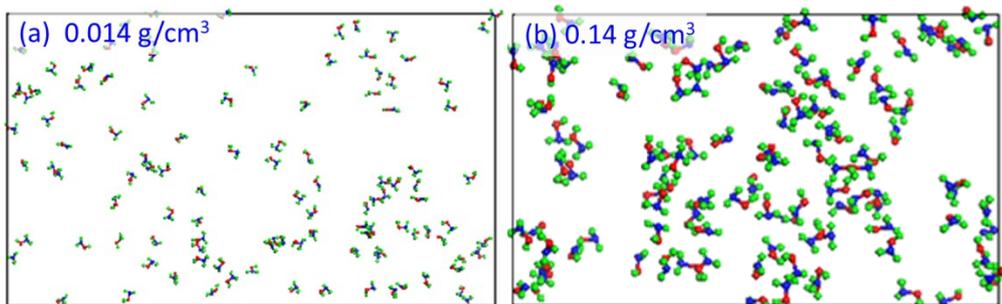
Fig. s3 Final snapshots at the 1000 K by the end of the simulation time of 30 ps with ReaxFF for Cases III (a) and II (b).

S3. The highest frequency reactions of pure HA and its aqueous solution heated at 1000 K.

Table S2. The highest frequency reactions within the initial 20 ps of pure HA (the reverse reactions are expunged).

Cases	Reactions	Frequencies
I: HA d=1.4g/cm^3	$H_2ON+OH \rightarrow H_3O_2N$	5
	$NH_2OH \rightarrow NH_2+OH$	5
	$NH_2OH+OH \rightarrow H_4O_2N$	5
	$2NH_2OH \rightarrow H_5ON_2+OH$	5
	$HNO \rightarrow H+NO$	5
	$OH+HNO \rightarrow H_2O+NO$	5
	$H_5ON_2 \rightarrow H_2ON+NH_3$	5
II: HA d=0.14g/cm^3	$NH_2OH \rightarrow NH_2+OH$	2
	$H_4N_2+2OH \rightarrow 2NH_2OH$	2
	$2NH_2OH \rightarrow H_2ON+NH_3+OH$	2
	$NH_2+NH_2OH \rightarrow H_5ON_2$	2
III: HA d=0.014g/cm^3	No Reactions	
IV: HA/water d=1.11g/cm^3	$NH_2OH+OH \rightarrow H_4O_2N$	3
	$NH_2OH+OH \rightarrow H_2O+H_2ON$	3
	$NH_2OH+HNO \rightarrow H_4ON+NO$	2
	$H+H_3O_2N \rightarrow H_4O_2N$	2
	$H_4ON \rightarrow H+NH_2OH$	2
	$OH+HNO \rightarrow H_2O+NO$	2

Table S3. The highest frequency reactions within the initial 30 ps of pure HA (the reverse reactions are expunged).

Cases	Reactions	Reaction No.	Frequencies
I: HA d=1.4g/cm^3	$OH+HON \rightarrow H_2O+NO$	(15)	5
	$NH_2OH+OH \rightarrow H_4O_2N$	(3)	5
	$H_2ON+OH \rightarrow H_3O_2N$	(13)	5
	$NH_2OH+OH \rightarrow H_2O+H_2ON$	(8)	5
	$NH_3+NH_2OH \rightarrow H_5N_2+OH$	(5)	5
	$H_2O_2N \rightarrow H_2O+NO$	(21)	5
	$NH_2OH \rightarrow H_2N+OH$	(12)	5
	$2NH_2OH \rightarrow H_5ON_2+OH$	(1)	5
II: HA d=0.14g/cm^3	$NH_2OH \rightarrow NH_2+OH$	(12)	4
	$N_2H_4+2OH \rightarrow 2NH_2OH$	(16)	2
	$2NH_2OH \rightarrow H_2ON+NH_3+OH$	(17)	2
	$2NH_2OH \rightarrow H_6O_2N_2$	(22)	2
	$NH_2+NH_2OH \rightarrow H_5ON_2$	(6)	2
	$H_5ON_2 \rightarrow N_2H_4+OH$	(23)	2
III: HA d=0.014g/cm^3	No Reactions		
IV: HA/water d=1.11g/cm^3	$NH_2OH \rightarrow NH_2+OH$	(12)	4
	$NH_2OH+OH \rightarrow H_2O+H_2ON$	(8)	4
	$H_2ON+NH_3 \rightarrow NH_2+NH_2OH$	(24)	3

S4. Comparisons of NBO charges and bond length of related molecules.
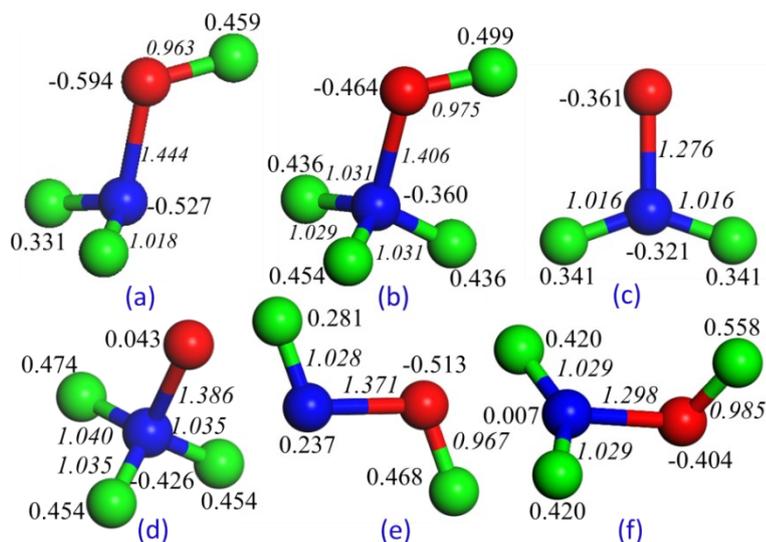
Fig. s4 Comparisons of NBO charges (in normal) and bond length (in italic) among HA (a), H-HA$^+$ (b), NH$_2$O (c), NH$_3$O$^+$ (d), NHOH (e) and NH$_2$OH$^+$ (f).

As to the above-mentioned strengthening of N-H and O-H bonds by protonation and the much more increase in BDE of the O-H bond than the N-H bond, they can be deduced by comparing the molecular stability of H-partitioned products from HA and H-HA$^+$. At first, regarding the enhanced strength of O-H and N-H bonds by protonation, we compare the molecular stability of NH$_2$O and NH$_3$O$^+$ (corresponding to the H-partitioned products by O-H break of HA and H-HA$^+$, respectively), and of NHOH and NH$_2$OH$^+$ (corresponding to the H-partitioned products by N-H break of HA and H-HA$^+$, respectively). Fig. s4(c) exhibits a shorter N-O bond, as well as shorter N-H bonds, than Fig. s4(d), implying the higher stability of NH$_2$O. The lower stability of NH$_3$O$^+$ suggests more energy required to break the O-H in H-HA$^+$, the larger BDE of the O-H bond. Even though the N-O bond in NH$_2$O (Fig. s4(e)) is longer than that in NH$_2$OH$^+$ (Fig. s4(f)) (1.371 vs. 1.298 Å), the electrostatic attraction between the O and N atoms in NH$_2$O are much stronger with more opposite charges, showing the lower stability of NH$_2$OH$^+$, or the larger BDE of the O-H bond in H-HA$^+$. Overall, both the N-H and O-H bonds are strengthened after protonation.

Furthermore, it is interesting to find that the strength order of N-H and O-H bonds is reversed

after protonation, i.e., the strength of the O-H bond increases much more than the N-H bond, as 168.3 versus 32.6 kJ/mol. This can also be understood by analyzing the molecular stability of H-partitioned products. The length of the N-O bond in Fig. s4(c) is shorter ~0.1 Å than that in Fig. s4(e), implying the higher stability of NH_2O in contrast to NHOH, i.e., the more energetically favored H-partition by O-H break. Thus, the higher BDE of the N-H bond relative to the O-H bond of HA in Fig. 8 (341 vs. 300.2 kJ/mol) is reasonable. Moreover, NH_3O^+ (Fig. s4(d)) possesses longer C-N bond length of ~0.09 Å than NH_2OH^+ (Fig. s4(f)); meanwhile, these two isomeric cations possess similar circumstances of electrostatic attraction between the N and O atoms of the N-O bonds, as $N^{-0.426}$-$O^{+0.043}$ vs. $N^{+0.007}$-$O^{-0.404}$. That is, NH_3O^+ is more energetically unstable than NH_2OH^+, or the O-H bond is stronger than the N-H bond in H-HA^+ (468.5 vs. 373.6 kJ/mol). In a word, the BDE of the O-H bond in H-HA^+ is larger than that in HA, while the BDE of the N-H bond in H-HA^+ is lower than that in HA. This order reversion suggests more BDE increasing of the O-H bond after protonation.

S5. Enthalpy changes of heterolytic cleavages of H-HA^+ and HA molecules.

H_3N^+-OH $\longrightarrow$ H^+ + H_2N-OH $\Delta H = 808.1$ kJ/mol

H_3N^+-OH $\longrightarrow$ H^+ + H_3N^+-O^- $\Delta H = 909.4$ kJ/mol

H_2N-OH $\longrightarrow$ H^+ + HN^--OH $\Delta H = 1653.3$ kJ/mol

H_2N-OH $\longrightarrow$ H^+ + H_2N-O^- $\Delta H = 1606.6$ kJ/mol
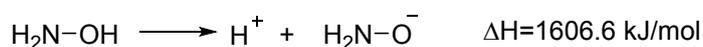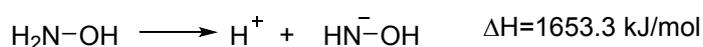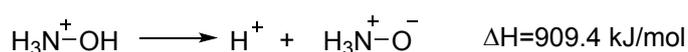
S6. References

(1) Fischer, N.; Izsák, D.; Klapötke, T.; Rappenglück, S.; Stierstorfer, J. *Chem. Eur. J.* **2012**, *18*, 4051 - 4062.

(2) Fischer, N.; Gao, L.; Klapötke, T.; Stierstorfer, J. *Polyhedron.* **2013**, *51*, 201-210.

(3) Klapötke, T.; Mayr, N.; Stierstorfer, J.; Weyrauther, M. *Chem. Eur. J.* **2014**, *20*, 1410- 1417.

(4) Fischer, D.; Klapötke, T.; Reymann, M.; Stierstorfer, J. *Chem. Eur. J.* **2014**, *20*, 6401-6411.

(5) Dippold, A.; Klapötke, T. *J. Am. Chem. Soc.* **2013**, *135*, 9931-9938.

(6)   Fischer, N.; Fischer, D.; Klapötke, T.; Piercey, D. G.; Stierstorfer, J. *J. Mater. Chem.* **2012**, *22*, 20418-20422.

(7)   Zhang, J. H.;Mitchell, L. A.; Parrish, D. A.; Shreeve, J. M. *J. Am. Chem. Soc.* **2015**, *137*,10532-10535.

(8)   Göbel, M.; Karaghiosoff, K.; Klapötke, T.; Piercey, D. G.; Stierstorfer, J. *J. Am. Chem. Soc.* **2010**, *132*, 17216-17226.

(9)   Zhang, J. H.; Shreeve, J. M. *J. Am. Chem. Soc.* **2014**, *136*, 4437-4445.

(10) Yin, P.; Parrish, D. A.; Shreeve, J. M. *J. Am. Chem. Soc.* **2015**, *137*, 4778-4786.

(11) Wang, R.; Xu, H.; Guo, Y.; Sa, R.; Shreeve, J. M. *J. Am. Chem. Soc.* **2010**, *132*, 11904-11905.

(12) Cheng, Y. G. *Chin. J. Explosive*, **1992**, *2*, 51-58.